Electronic Supplementary Information

Stacking-dependent tetracolour luminescence and mechanofluorochromic properties of an isoquinoline derivative with aggregation-induced emission

Yating Chen,[1‡] Bo Wang,[2‡] Yunxiang Lei,[1*] Yunbing Zhou,[1] Yang Guo,[2*] Miaochang Liu,[1] Wenxia Gao,[1] Xiaobo Huang[1*] and Huayue Wu[1]

[1] College of Chemistry and Materials Engineering, Wenzhou University, Wenzhou 325035, P. R. China

E-mail: yunxianglei@wzu.edu.cn (Y. Lei), xiaobhuang@wzu.edu.cn (X. Huang)

[2] Qingdao Institute for Theoretical and Computational Sciences, Institute of Frontier and Interdisciplinary Science, Shandong University, Qingdao 266237, P. R. China

E-mail: yang.guo@sdu.edu.cn (Y. Guo)

‡ These authors contributed equally to this work

Contents:

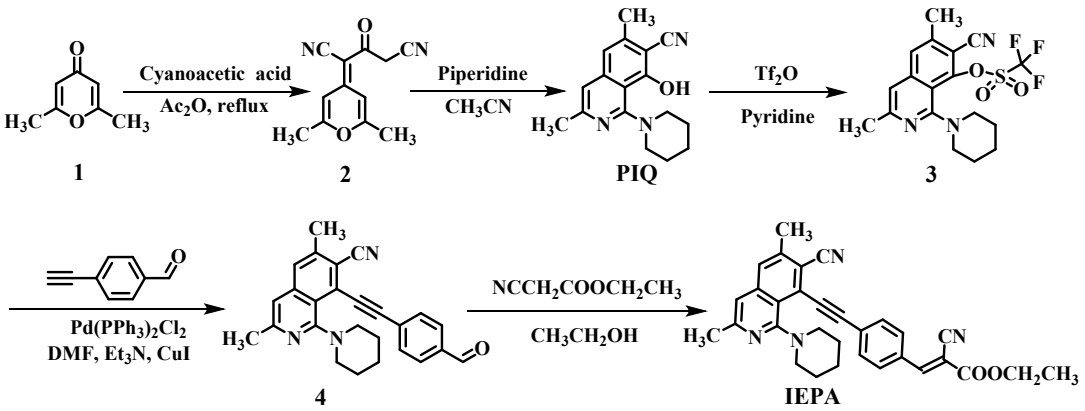

Scheme S1 Synthetic route of **IEPA**.

1. Experimental

Measurements and materials

^{1}H NMR and ^{13}C NMR spectra were tested on a Bruker DRX 500 NMR spectrometer using $CDCl_3$ as the solvent. Melting points were obtained from WRS-1B digital melting point meter (uncorrected). Fourier transform infrared (FT-IR) spectra were obtained from a Nexus 870 FT-IR spectrometer. High-resolution electrospray ionization (HRMS-ESI) mass spectra were obtained from a Hitachi Nano Frontier LD spectrometer. X-Ray powder diffraction (XRD) patterns were obtained from an Empyrean X-ray diffraction instrument. Fluorescence spectra were obtained using a Cary Eclipse fluorescence spectrophotometer. The absolute fluorescence quantum yields and fluorescence lifetime decays were performed using Jobin Yvon Horiba FluoroMax-4 fluorometer. UV-vis absorption spectra were conducted on a UV-3600 Shimadzu spectrophotometer. Differential scanning calorimetry (DSC) experiments were obtained from a TA-DSC Q2000 at a heating rate of 10 °C/min. Fluorescence microscopic images were obtained using a Leica DMI3000B inverted optical microscope. Single-crystal X-ray data were collected with graphite-monochromated MoKα radiation on a Bruker-Nonius Smart Apex CCD diffractometer. 2,6-Dimethyl-4-pyranone (**1**), acetic anhydride, cyanoacetic acid, piperidine trifluoromethanesulfonic anhydride (Tf_2O), 4-ethynylbenzaldehyde, $Pd(PPh_3)_2Cl_2$, and ethyl 2-cyanoacetate were commercially available and used directly. 2-(2,6-Dimethyl-4*H*-pyran-4-ylidene)-3-oxopentanedinitrile (**2**), 8-hydroxy-3,6-dimethyl-1- (piperidin-1-yl)isoquinoline-7-carbonitrile (**PIQ**), and 7-cyano-3,6-dimethyl-1-(piperidin-1- yl)isoquinolin-8-yl trifluoromethanesulfonate (**3**) were synthesized using compound **1** as the starting material according to the previous literature.[1]

Synthesis of 8-((4-formylphenyl)ethynyl)-3,6-dimethyl-1-(piperidin-1-yl)isoquinoline- 7-carbonitrile (4)

A mixture of compound **3** (826.8 mg, 2.0 mmol), 4-ethynylbenzaldehyde (390.5 mg, 3.0 mmol), CuI (22.9 mg, 0.12 mmol), $Pd(PPh_3)_2Cl_2$ (84.0 mg, 0.12 mmol), triethylamine (6 mL), and *N*,*N*-dimethylformamide (6 mL) was stirred for 12 h at 100°C under a N_2 atmosphere. The reaction mixture

was allowed to cool to room temperature and then poured into water. The mixture was extracted three times with dichloromethane. The organic solvent was evaporated by decompression and the residue was passed through a silica gel column chromatography (ethyl acetate: petroleum ether = 1:8, v:v) to afford a yellow solid (594.2 mg, 75.5% yield). M. p. 230.2-231.0°C. ^{1}H NMR ($CDCl_3$, 500 MHz): δ 10.04 (s, 1H), 7.92 (d, J = 8.0 Hz, 2H), 7.86 (d, J = 8.0 Hz, 2H) , 7.42 (s, 1H), 6.87 (s, 1H), 3.61 (br, 2H), 3.15 (br, 2H), 2.62 (s, 3H), 2.51 (s, 3H), 1.81-1.48 (m, 6H) ppm. ^{13}C NMR ($CDCl_3$, 125 MHz): 191.1, 160.5, 153.1, 141.6, 139.5, 136.0, 132.4, 129.7, 128.9, 127.2, 125.8, 117.5, 116.2, 116.0, 111.8, 99.7, 91.5, 53.1, 25.4, 24.5, 24.2, 20.9 ppm. HRMS (ESI) m/z: $[M+H]^+$ calculated for $C_{26}H_{24}N_3O$, 394.1914; found, 394.1918.

Synthesis of ethyl (*E*)-2-cyano-3-(4-((7-cyano-3,6-dimethyl-1-(piperidin-1-yl)isoquinolin-8-yl)ethynyl)phenyl)acrylate (IEPA)

The mixture of compound **4** (399.5 mg, 1.0 mmol), ethyl 2-cyanoacetate (452.4 mg, 4.0 mmol), and ethanol (10 mL) was stirred at 80°C for 8 h under a N_2 atmosphere. After the reaction was completed, a large amount of solid precipitated after cooling to room temperature. Under vacuum condition, the precipitate was filtered and washed with ethanol for three times to afford an orange solid (420.7 mg, 86.1%). M. p. 165.0-166.0°C. ^{1}H NMR ($CDCl_3$, 500 MHz): 8.24 (s, 1H) , 8.05 (d, J = 8.0 Hz, 2H), 7.82 (d, J = 8.5 Hz, 2H), 7.44 (s, 1H), 6.88 (s, 1H), 4.40 (q, J = 7.0 Hz, 2H), 3.62 (br, 2H), 3.16 (br, 2H), 2.63 (s, 3H), 2.53 (s, 3H), 1.82-1.49 (m, 6H), 1.41 (t, J = 7.0 Hz, 3H) ppm. ^{13}C NMR ($CDCl_3$, 125 MHz): δ 162.2, 160.4, 153.5, 153.1, 141.5, 139.4, 132.4, 131.6, 131.0, 127.7, 127.2, 125.6, 117.5, 116.1, 116.0, 115.3, 111.8, 103.5, 99.7, 91.9, 62.8, 53.0, 25.3, 24.4, 24.2, 20.8, 14.1 ppm. FT-IR (KBr, cm^{-1}): 2938, 2849, 2824, 2221, 1725, 1717, 1591, 1534, 1371, 1258, 1206, 1075, 847, 825, 764. HRMS (ESI) m/z: $[M+H]^+$ calculated for $C_{31}H_{29}N_4O_2$, 489.2285; found, 489.2277.

Solid-state time-resolved emission decay parameters of IEPA under different conditions

The solid-state fluorescence decay parameters of **IEPA** under different conditions are obtained from the following equation: $I = A_1\exp(-t/\tau_1)+A_2\exp(-t/\tau_2)$.[2] Herein, τ_1 and τ_2 are the lifetimes of the shorter-lived and longer-lived species, respectively, and A_1 and A_2 are their respective amplitudes. The weighted mean lifetime $<\tau>$ is obtained from the following equation: $<\tau> = (A_1\tau_1+A_2\tau_2)/(A_1+A_2)$. The radiative rate constant k_f and non-radiative rate constant k_{nr} are obtained from the following equations of $k_f = \Phi_F/<\tau>$ and $k_{nr} = (1-\Phi_F)/<\tau>$, respectively.[3]

2. Computational details

Chemical model construction

To simulate the crystalline effect without periodic boundary condition, an active site model containing molecules in a 3 × 2 × 2 supercell is constructed for each polymorph based on the crystal structure. The PM7, a semi-empirical QM method in MOPAC,[4] is used to optimize the position of hydrogen atoms. For the models used in excited states calculations, only the two parallel-stacked molecules in

the center of the active site are chosen as the QM region. The remaining molecules are approximated as external point charges. The point charge of each atom in a polymorph calculation is computed self-consistently using the natural population analysis of wave function computed at M062X/Def2-SVP level.

Excited states calculations

To simulate the UV-Vis spectra of the four IEPA polymorphs, 10 lowest singlet excited states are computed by TD-DFT at M062X/Def2-TZVP level embedded in the external point charge environment. For comparison, the TD-DFT results without external point charges are performed as well. The UV-Vis spectra without and with external point charges are given in Fig. 9A and Fig. 9B, respectively. All calculations are performed using Gaussian16 package.[5]

References

1 Y. Chen, X. Zhang, M. Wang, J. Peng, Y. Zhou, X. Huang, W. Gao, M. Liu and H. Wu, *J. Mater. Chem. C*, 2019, **7**, 12580–12587.

2 X. Zhang, Z. Chi, B. Xu, C. Chen, X. Zhou, Y. Zhang, S. Liu and J. Xu, *J. Mater. Chem.*, 2012, **22**, 18505–18513.

3 B. Fang, M. Chu, Z. Wu, Y. Shi, Y. S. Zhao and M. Yin, *J. Mater. Chem. C*, 2019, **7**, 4434–4440.

4 MOPAC2016, J. Stewart, Stewart Computational Chemistry, Colorado Springs, CO, USA, HTTP://OpenMOPAC.net (2016).

5 M. J. Frisch, G. W. Trucks, H. B. Schlegel, G. E. Scuseria, M. A. Robb, J. R. Cheeseman, G. Scalmani, V. Barone, G. A. Petersson, H. Nakatsuji, X. Li, M. Caricato, A. V. Marenich, J. Bloino, B. G. Janesko, R. Gomperts, B. Mennucci, H. P. Hratchian, J. V. Ortiz, A. F. Izmaylov, J. L. Sonnenberg, D. Williams-Young, F. Ding, F. Lipparini, F. Egidi, J. Goings, B. Peng, A. Petrone, T. Henderson, D. Ranasinghe, V. G. Zakrzewski, J. Gao, N. Rega, G. Zheng, W. Liang, M. Hada, M. Ehara, K. Toyota, R. Fukuda, J. Hasegawa, M. Ishida, T. Nakajima, Y. Honda, O. Kitao, H. Nakai, T. Vreven, K. Throssell, J. A. Montgomery, Jr., J. E. Peralta, F. Ogliaro, M. J. Bearpark, J. J. Heyd, E. N. Brothers, K. N. Kudin, V. N. Staroverov, T. A. Keith, R. Kobayashi, J. Normand, K. Raghavachari, A. P. Rendell, J. C. Burant, S. S. Iyengar, J. Tomasi, M. Cossi, J. M. Millam, M. Klene, C. Adamo, R. Cammi, J. W. Ochterski, R. L. Martin, K. Morokuma, Ö. Farkas, J. B. Foresman, and D. J. Fox, *Gaussian 16*, *Revision C.01*, Gaussian, Inc., Wallingford CT, 2016.

3. Figures and tables

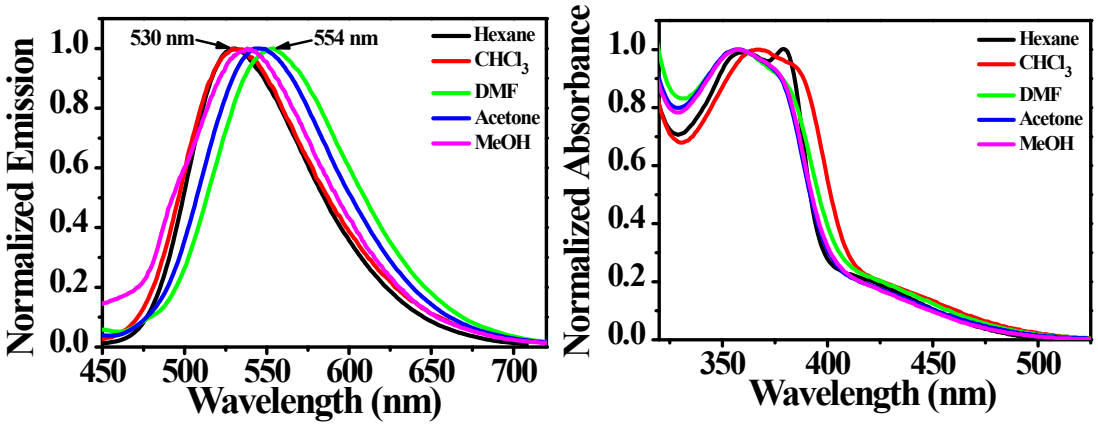

Fig. S1 Normalized fluorescence (left) and absorption (right) spectra of **IEPA** in different solvents (λ_{ex}: 430 nm). Concentration: 1×10^{-5} mol/L.

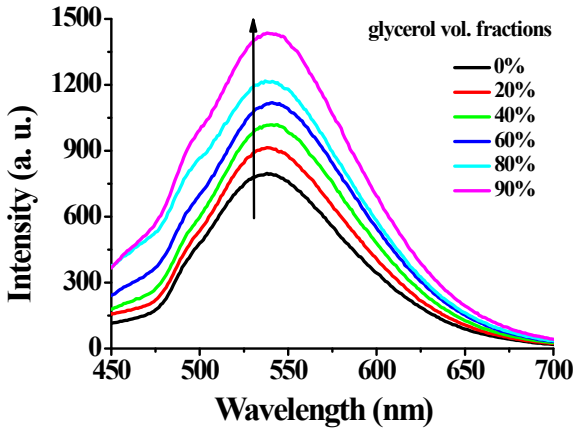

Fig. S2 Fluorescence spectra of **IEPA** in glycerol-methanol mixtures with different glycerol volume fractions (λ_{ex}: 430 nm).

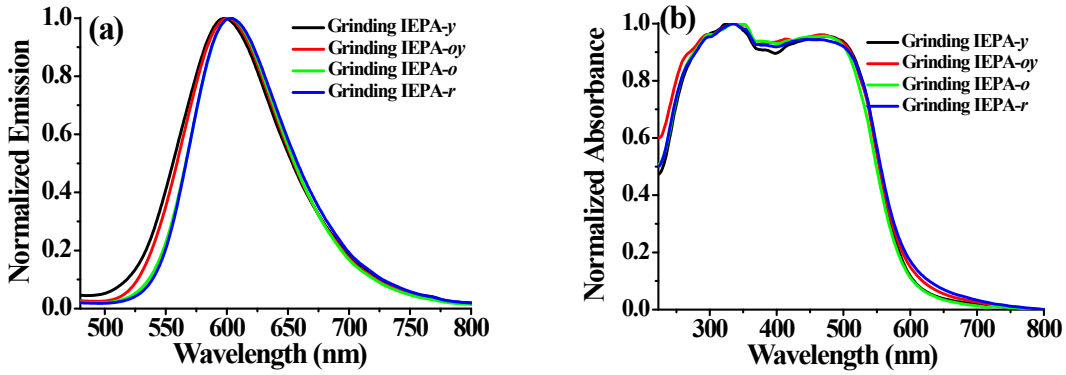

Fig. S3 Normalized fluorescence (a) and absorption (b) spectra of the ground samples obtained from the polymorphs of **IEPA** (λ_{ex}: 440 nm).

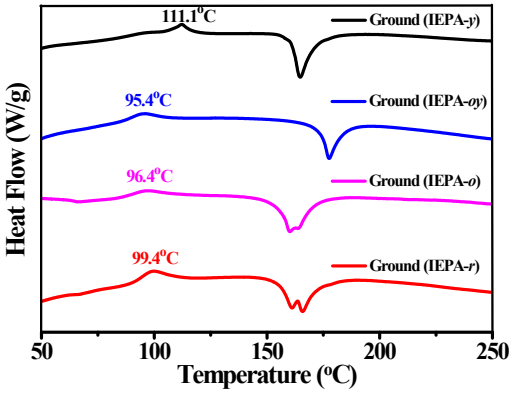

Fig. S4 DSC curves of the ground samples of **IEPA-*y***, **IEPA-o*y***, **IEPA-*o***, and **IEPA-*r***.

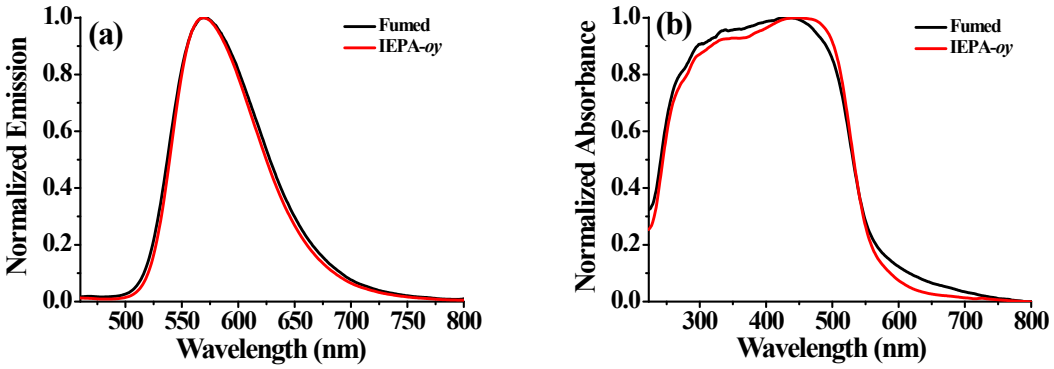

Fig. S5 Comparison of fluorescence (a) and absorption (b) spectra of **IEPA-o*y*** and the fumed sample obtained from the ground samples of the four polymorphs (λ_{ex}: 440 nm).

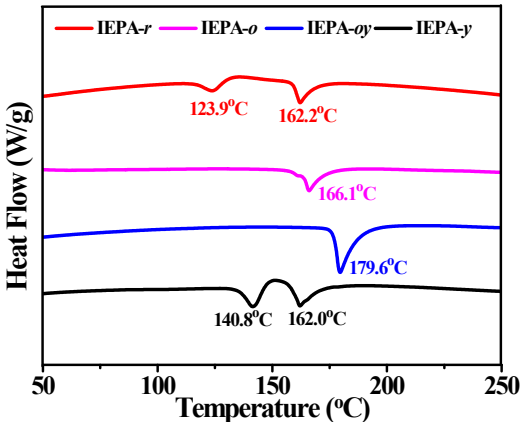

Fig. S6 DSC curves of **IEPA-*y***, **IEPA-o*y***, **IEPA-*o***, and **IEPA-*r***.

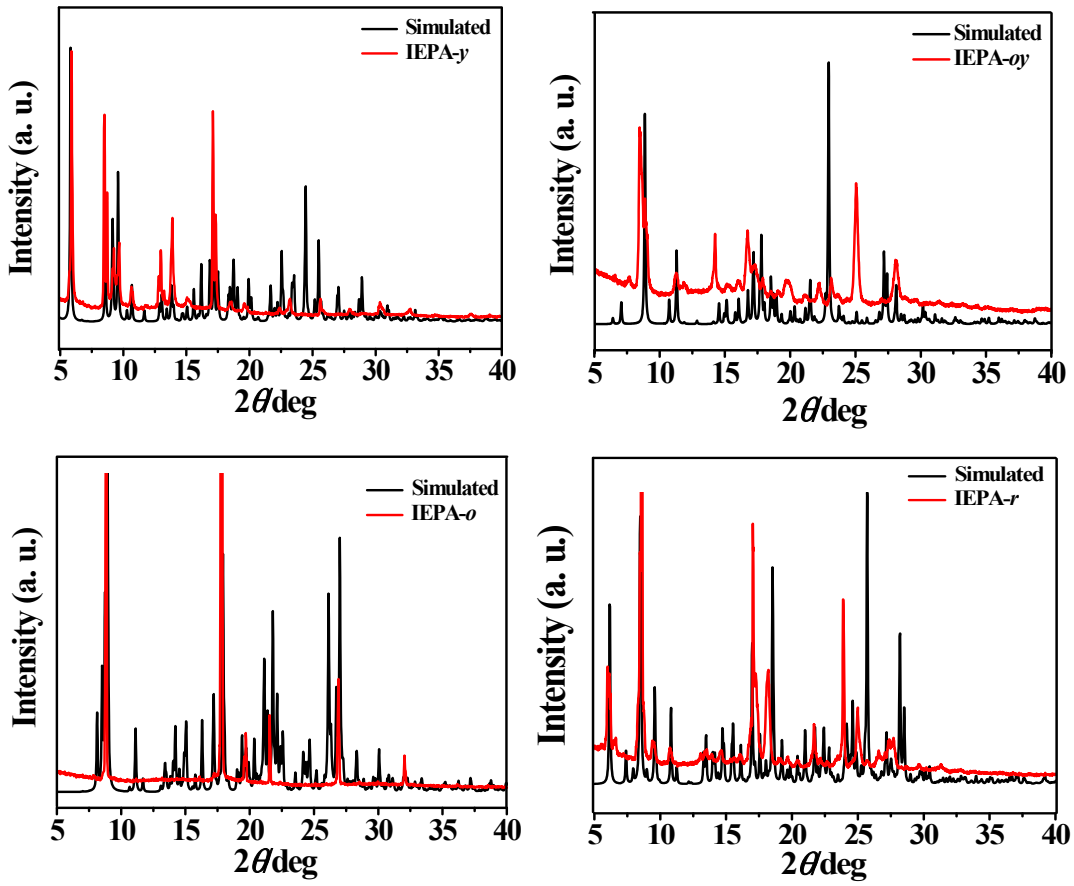

Fig. S7 Comparison of experimental XRD curves and the simulated XRD curves obtained from the corresponding single crystals of **IEPA-*y***, **IEPA-o*y***, **IEPA-*o***, and **IEPA-*r***.

Table S1 Crystal data and details of collection and refinement of the polymorphs of **IEPA**.

	IEPA-*y*	**IEPA-*oy***	**IEPA-*o***	**IEPA-*r***
CCDC (no.)	2060702	2060705	2060704	2060703
Formula weight	488.57	488.57	1062.07	1023.21
Temperature (K)	273.15	293(2)	293(2)	193(2)
Crystal system	Monoclinic	Monoclinic	Triclinic	Monoclinic
Space group	$P\bar{1}$ 2(1)/*c*1	*P* 2(1)/*c*	$P\bar{1}$	*P* 2(1)/*n*
Z	8	4	2	4
D_{calcd} [Mg/m^3]	1.193	1.249	1.266	1.241
F (000)	2064	1032	1116	2168
θ range [°]	2.371-24.998	2.474-25.499	2.067-25.500	2.492- 25.498
R_1 [I>2σ(I)]	0.0947	0.0531	0.0657	0.0643
wR_2 [I>2σ(I)]	0.2580	0.1124	0.1556	0.1470
a [Å]	20.8149(17)	6.3103(4)	11.2380(3)	13.3441(5)
b [Å]	6.8015(5)	25.0008(17)	13.7013(4)	20.8744(8)
c [Å]	38.825(3)	16.5723(12)	20.3358(5)	19.9767(8)
α [deg]	90	90	81.7010(10)	90
β [deg]	98.107(2)	96.440(2)	75.4480(10)	100.0940(10)
γ [deg]	90	90	67.0470(10)	90
V [Å^3]	5441.6(7)	2598.0(3)	2787.02(13)	5478.4(4)
GOF	1.682	1.058	1.009	1.030
R (int)	0.0950	0.0783	0.0506	0.0623
No. of reflcns collected	94000	37128	53688	58304
No. of unique reflcns	9525	4837	10358	10177
R_1 (all data)	0.1310	0.1082	0.1031	0.1065
wR_2 (all data)	0.2763	0.1437	0.1852	0.1752

4. Spectra of NMR

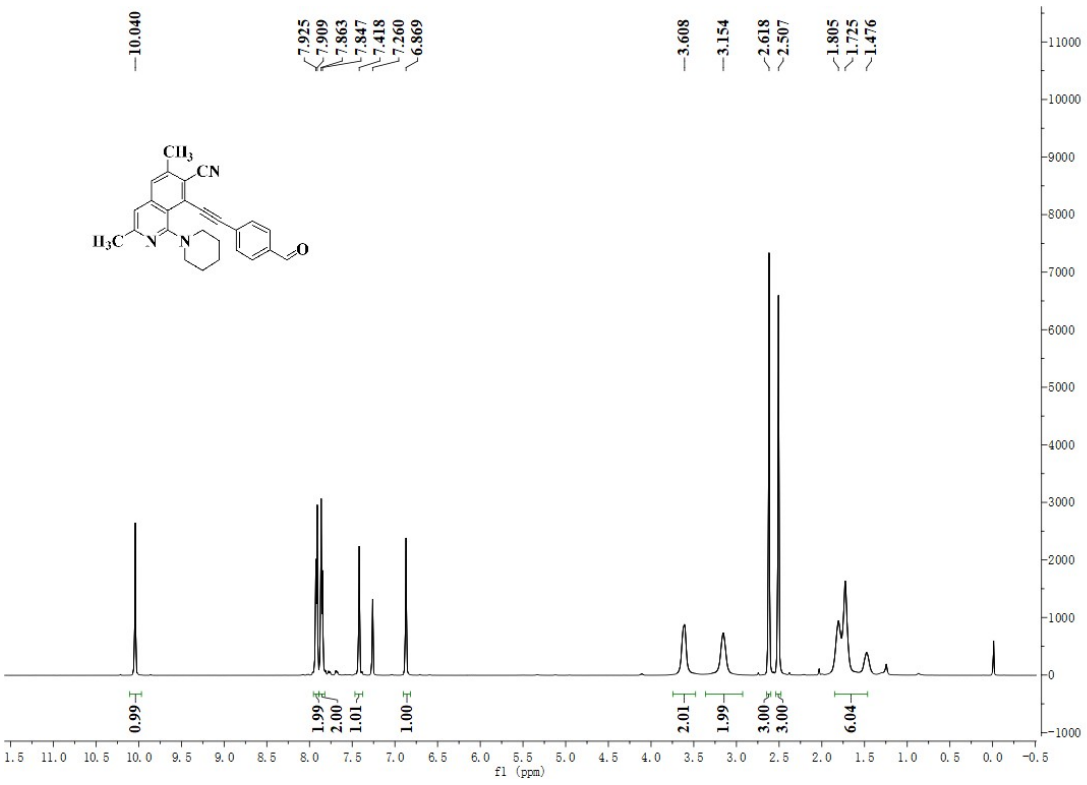

Fig. S8 ^{1}H NMR of compound **4** ($CDCl_3$, 500 MHz).

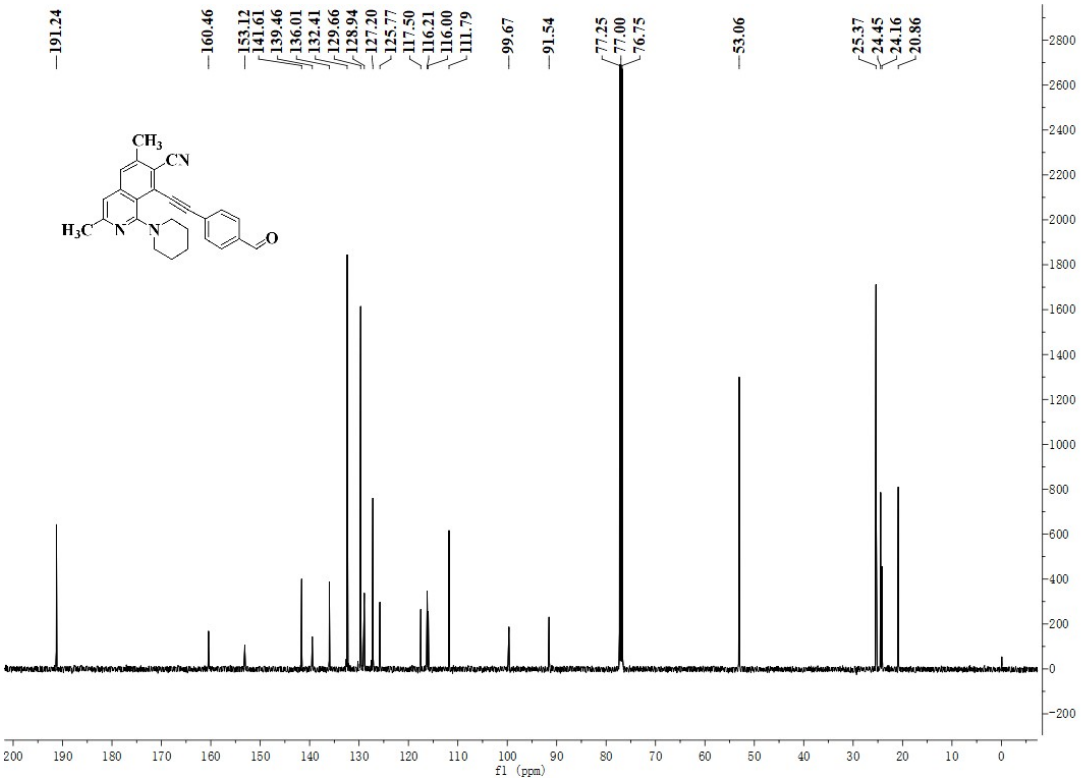

Fig. S9 ^{13}C NMR of compound **4** ($CDCl_3$, 125 MHz).

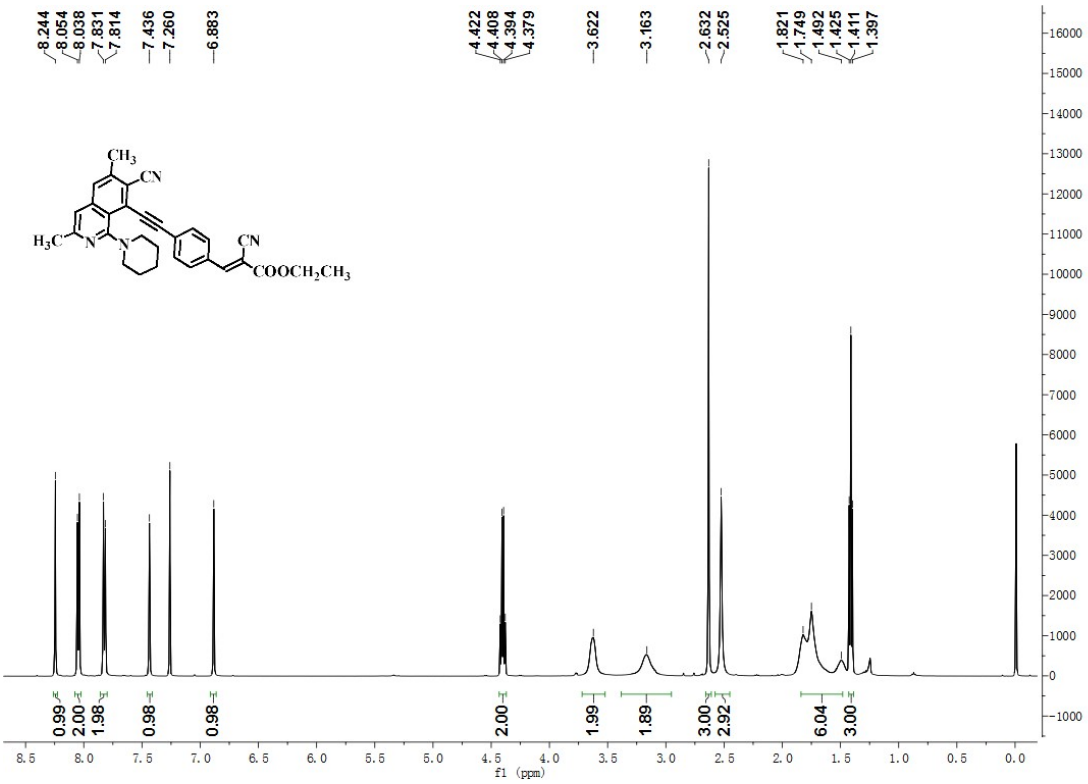

Fig. S10 ^{1}H NMR of **IEPA** ($CDCl_3$, 500 MHz).

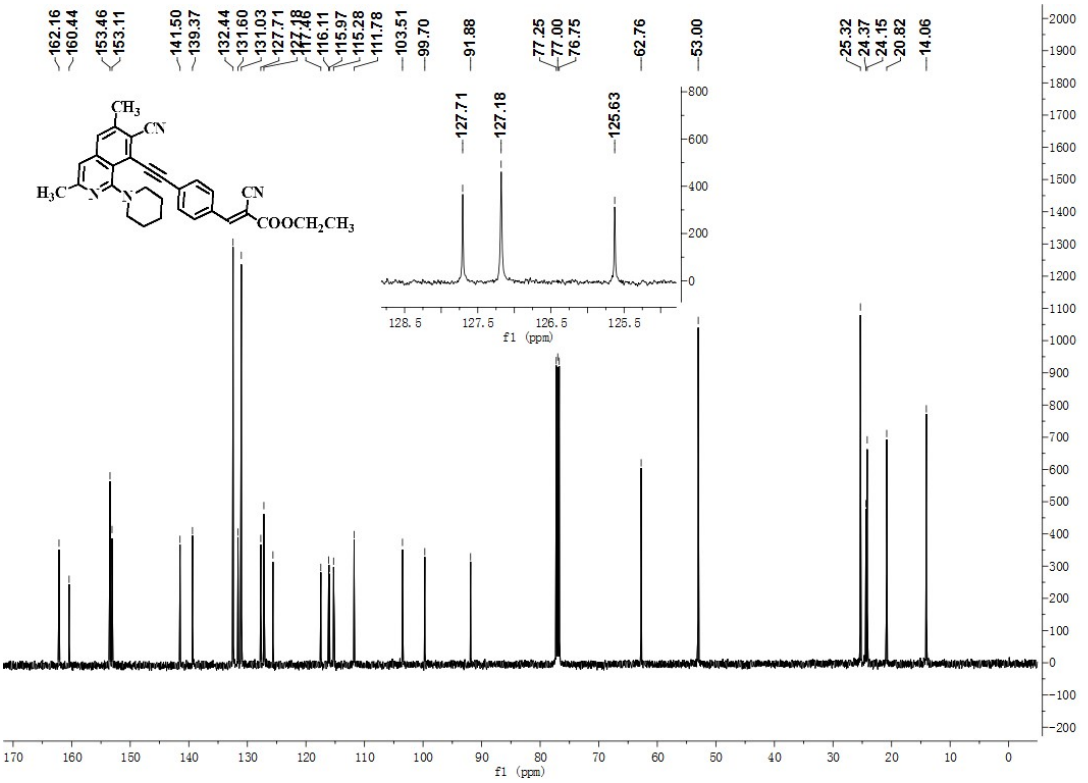

Fig. S11 ^{13}C NMR of **IEPA** ($CDCl_3$, 125 MHz).